

doi:10.7515/JEE201506002

基于“平均值概念”的“残差示踪法” ——黄土高原降水重建的应用

周卫健^{1,2,3,4}, 陈茂柏^{1,2}, 孔祥辉^{1,2}, 鲜锋^{1,2}, 杜雅娟^{1,2},
武振坤^{1,2}, 宋少华^{1,2}, 康志海^{1,2}

(1. 中国科学院地球环境研究所 黄土与第四纪地质国家重点实验室, 陕西省加速器质谱技术及
应用重点实验室, 西安 710061; 2. 西安加速器质谱中心, 西安 710061;
3. 北京师范大学, 北京 100875; 4. 西安交通大学 人居环境与建筑工程学院, 西安 710049)

摘要: 本文对定量重建黄土高原降水的传统方法进行了回顾分析, 提出了利用新发展的“残差示踪法”定量重建黄土高原古降水变化的两种新方法。一种是利用黄土磁化率和粉尘通量指标的关系进行降水重建的磁化率方法 (*SUS-approach*), 另一种是利用黄土¹⁰Be浓度与¹⁰Be产率和粉尘通量指标的关系进行降水重建的¹⁰Be方法 (*¹⁰Be-approach*)。上述两种方法定量重建的洛川地区 13 万年以来降水变化曲线高度一致, 但与前人利用现代观测数据建立的气候回归方程等传统方法重建的降水记录具有明显的差异。本文所建立的降水曲线具有明显的细节特征, 揭示了粉尘稀释作用对降水指标的影响, 显示了该方法的优势。文章同时指出, “残差示踪法”的数学涵义是基于“平均值概念”(MVC), 并对此从统计学角度进行了论证。最后, 就本文所提出的运用线性回归后的残差进行示踪的新方法与传统的示踪方法之差异作了对比分析。

关键词: 黄土高原; *SUS-approach*; *¹⁰Be-approach*; 平均值概念 (MVC); 残差示踪法; 古降水
中图分类号: P532 **文献标志码:** A **文章编号:** 1674-9901(2015)06-0382-11

“Mean Value Concept” based “Residual Trace Approach” — application to paleoprecipitation reconstruction over the Chinese Loess Plateau

ZHOU Wei-jian^{1,2,3,4}, CHEN Mao-bai^{1,2}, KONG Xiang-hui^{1,2}, XIAN Feng^{1,2}, DU Ya-juan^{1,2},
WU Zhen-kun^{1,2}, SONG Shao-hua^{1,2}, KANG Zhi-hai^{1,2}

(1. State Key Laboratory of Loess and Quaternary Geology and Shaanxi Key Laboratory of Accelerator Mass Spectrometry
Technology and Application, Institute of Earth Environment, Chinese Academy of Sciences, Xi'an 710061, China;
2. Xi'an Accelerator Mass Spectrometry Center, Xi'an 710061, China; 3. Beijing Normal University, Beijing 100875, China;
4. School of Human Settlements and Civil Engineering, Xi'an Jiaotong University, Xi'an 710049, China)

Abstract: The traditional trace methods for paleoprecipitation reconstruction over Chinese Loess Plateau are first analyzed. Then, two practical applications of the newly developed “Residual Trace Approach” to quantitatively reconstruct the paleoprecipitation over the Chinese Loess Plateau are described. One is the “*SUS-approach*” that uses paired measurements of magnetic susceptibility and dust flux in loess-paleosol sediments as proxies, the other is the “*¹⁰Be-approach*” that uses both atmospheric ¹⁰Be production rate and loess dust flux as proxies. The reconstructed precipitation curves of the past 130 ka over Luochuan loess plateau site by the two approaches are highly correlated. However, they are different to some extent from the other precipitation curves calculated by the

Received Date: 2015-09-29

Foundation Item: National Basic Research Program of China (2013CB955904); National Natural Science Foundation of China (41230525); MOST (Ministry of Science and Technology) Special Fund for State Key Laboratory of Loess and Quaternary Geology.

Corresponding Author: ZHOU Wei-jian, E-mail: weijian@loess.llqg.ac.cn

individual climofunctions of the previous studies using traditional trace methods, and the detailed variations evident in the new approach offer an advantage over the traditional methods in revealing the dust dilution effect on the reconstructed precipitation. Furthermore, it is pointed out that the mathematical connotation of the "Residual Trace Approach" is equivalent to the "Mean Value Concept (MVC)" which is further explained from a statistical point of view. Finally, the difference of the "Residual Trace Approach" from the traditional trace method is compared.

Key words: Chinese Loess Plateau; *SUS*-approach; ^{10}Be -approach; Mean Value Concept; Residual Trace Approach; paleoprecipitation

1 Background of the traditional approach for paleoprecipitation reconstruction over the Chinese Loess Plateau

The magnetic susceptibility records in Chinese loess-paleosols are very similar to the $\delta^{18}\text{O}$ records from deep-sea sediments. This similarity led to the suggestion that magnetic susceptibility records from loess-paleosols could be used for paleoclimate change research (Kukla et al, 1988). For more than two decades, a number of studies (Maher et al, 1994; An and Sun, 1995; Sun et al, 1995; Han et al, 1996; Porter et al, 2001) have pursued this approach, with magnetic susceptibility as a proxy of paleoprecipitation over the Chinese Loess Plateau (CLP). These studies took important steps towards the spatial and temporal reconstruction of paleoprecipitation over the CLP. However, it becomes clear that the magnetic

susceptibility signal in loess includes a dustfall induced susceptibility from the dust source regions that is not related to precipitation, and that the rainfall-induced pedogenic susceptibility is controlled by chemical/biochemical pedogenic processes. Because it is not yet possible to collect information on all of the variables involved in pedogenic susceptibility, they cannot be quantitatively accounted for through conventional regression analysis (Porter et al, 2001). Therefore most studies have considered precipitation as the dominant factor that controls the pedogenic processes, and have adopted different simplifying assumptions to rule out other non-precipitation factors, and to reconstruct paleoprecipitation. These studies have given rise to a diverse set of climofunctions and results (Maher et al, 1994; An and Sun, 1995; Sun et al, 1995; Han et al, 1996; Porter et al, 2001) (Tab.1).

Tab.1 Different types of climofunction in published papers

Researchers	Climofunction
Maher et al (1994)	$P = 222 + 199 \log(SUS)$
Sun et al (1995)	$P = -415.593 + 215.778 \ln(SUS)$
Han et al (1996)	$P = -22.706 + 11554S - 6.7166 \times 10^{-2}S^2 + 1.8684 \times 10^{-4}S^3 - 1.9264 \times 10^4$
Porter et al (2001)	$MS = (5.65E-4 \times MAP^{2.15} + 400) / T$

Note: P and MAP represent the precipitation ($\text{mm} \cdot \text{a}^{-1}$), SUS , S and MS represent the loess magnetic susceptibility ($10^{-8} \text{ m}^3 \cdot \text{kg}^{-1}$), T is the loess thickness (m).

All of the climofunctions cited in Tab.1, with the exception of Porter et al (2001), were established using a best fit between present (most recent 10~30 years) precipitation and total magnetic susceptibility (or pedogenic susceptibility) in the modern soil (near surface) from different locations, without consideration of the dust dilution effect. Namely, all these papers through burdensome work have ruled out all non-precipitation factors in regression calculations,

leaving the latest 10~30 years' precipitation alone. As a result, the effect of non-precipitation factors, including dustfall-induced susceptibility $SUS(D)$ and the dilution effect (Kukla et al, 1988; Porter et al, 2001) of the slow dust deposition during pedogenesis (An and Sun, 1995; Porter et al, 2001), have altogether been taken as the rainfall-related composition to be fitted with the measured present precipitation P in their regression, which has resulted in that the inherent

linear correlation between the precipitation and the pedogenic susceptibility (Beer et al, 1993; Heller et al, 1993; An and Sun, 1995; Shen et al, 2000; Zhou et al, 2007a) was incorporated into a nonlinear climofunction (polynomial type or logarithmic type) depending on the local and temporal climate conditions being considered (Tab.1). These different types of nonlinear climofunctions did not achieve a perfect correlation between precipitation and pedogenic susceptibility in nature as they only reflected the best fit between the present precipitation and near surface susceptibility for a specific locality over the past 10~30 years.

A basic question that arises from the aforementioned approach is whether climofunctions from the latest 10~30 years' data can be extended to include past glacial and interglacial periods. Such an approach implies that all non-precipitation factors have been constant or have negligible changes from glacial and interglacial ages through the present. This is obviously not a valid assumption. For example, Fig.1a shows

the dust flux (D) from the Louchuan loess profile for the past 130 ka, with a relative standard deviation $RSD = 25\%$. This record features an abrupt change in dust flux at circa 80 ka that reached up to 200%. The large fluctuation of the dust flux indicates that it is inappropriate to apply the climofunctions in Table 1 through this interval. This includes the formula of Porter et al (2001), which accounts for the dust dilution effect, but still refers to recent accumulation rates.

In addition to the susceptibility-based approach for paleoprecipitation reconstruction, Heller et al (1993) exploited a " ^{10}Be -Susceptibility similarity" approach to extract the pedogenic susceptibility. In their approach, they used both susceptibility and ^{10}Be to reconstruct regional paleorainfall in the CLP (Beer et al, 1993; Heller et al, 1993; Shen et al, 2000). However, their approach did not consider both dust flux variations and ^{10}Be changes associated with geomagnetic field changes. The latter account for 10%~20% of the total ^{10}Be signal.

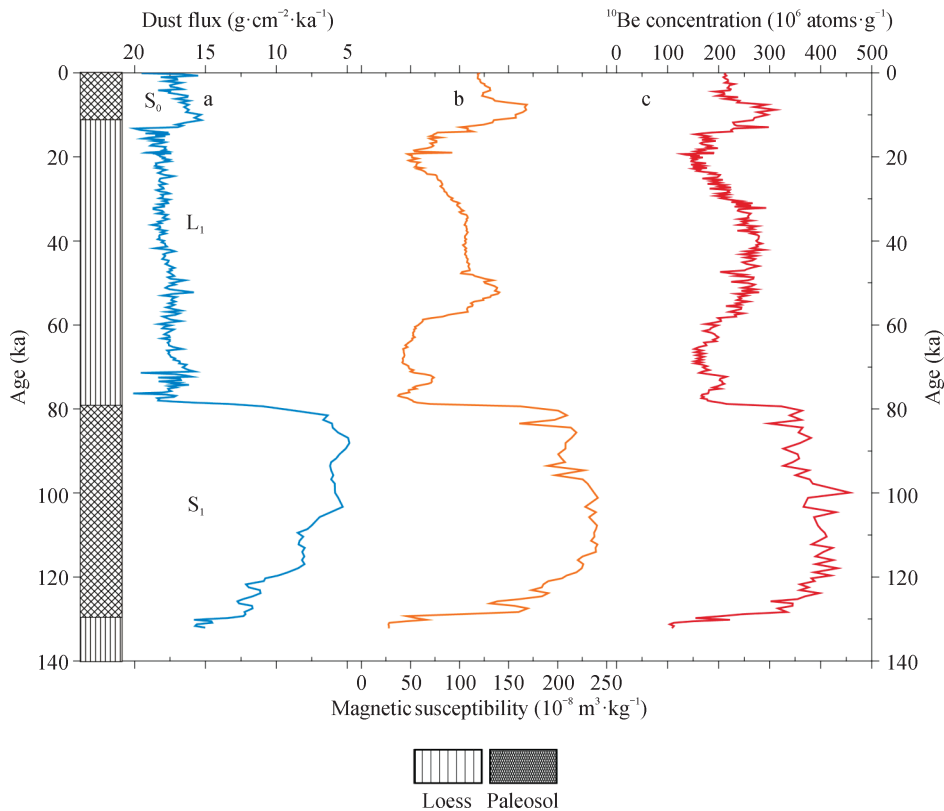


Fig.1 The dust flux D (a), magnetic susceptibility (b), ^{10}Be concentration (c) for the past 130 ka of the Louchuan loess profile. The RSD (relative standard deviation) of D , i.e. the ratio of the mean root square of the fluctuation ΔD to their average value \bar{D} , is 25%, an abrupt change occurred at circa 80 ka. The high magnetic susceptibility during 80~110 ka was formed by a combination of high precipitation and low dust flux (Fig.1a) rather than by high precipitation alone.

Authors have used the correlation between ^7Be in modern precipitation (Wallbrink and Murray, 1994; Ishikawa et al, 1995; Caillet et al, 2001) and tropospheric $^{10}\text{Be}/^7\text{Be}$ ratio to derive quantitative estimates of the past 80 ka precipitation over the Luochuan profile (Zhou et al, 2007a). The results were comparable to speleothem $\delta^{18}\text{O}$ records from Dongge and Hulu caves (Wang et al, 2001, 2008), however the approach relies the correlation with ^7Be which again is only available from modern observations. Hence the method cannot fully account

for geomagnetic field changes and dust dilution effects that one may expect when extending a model to the past 80 ka.

Hence, a quantitative reconstruction of paleoprecipitation remains a crucial goal towards understanding changes in East Asia Monsoon intensity through time. Here we introduce a new method to reconstruct paleoprecipitation by using loess magnetic susceptibility and ^{10}Be records.

In order to make it clear, we explain a few terms used in the text as following (Tab.2).

Tab.2 The explanation of terms used in this study

Terms	Explanation (units)
$SUS(M)$	Measured magnetic susceptibility in loess ($10^{-8} \text{ m}^3 \cdot \text{kg}^{-1}$)
$SUS(D)$	Magnetic susceptibility component carried in dust ($10^{-8} \text{ m}^3 \cdot \text{kg}^{-1}$)
$SUS(P)$	Magnetic susceptibility component related to the precipitation ($10^{-8} \text{ m}^3 \cdot \text{kg}^{-1}$)
$SUS(M)_e$	Magnetic susceptibility estimated by linear regression analysis ($10^{-8} \text{ m}^3 \cdot \text{kg}^{-1}$)
$\text{Be}(M)$	Measured ^{10}Be concentration in loess ($10^6 \text{ atoms} \cdot \text{g}^{-1}$)
$\text{Be}(D)$	^{10}Be concentration carried in dust ($10^6 \text{ atoms} \cdot \text{g}^{-1}$)
$\text{Be}(P)$	^{10}Be concentration related to the precipitation ($10^6 \text{ atoms} \cdot \text{g}^{-1}$)
$\text{Be}(M)_e$	^{10}Be concentration estimated by linear regression analysis ($10^6 \text{ atoms} \cdot \text{g}^{-1}$)
D	Dust flux ($\text{g} \cdot \text{cm}^{-2} \cdot \text{ka}^{-1}$)
P	Precipitation ($\text{mm} \cdot \text{a}^{-1}$)
Pr	^{10}Be production rate

2 Application of the “Residual Trace Approach” to the paleoprecipitation reconstruction over the past 130 ka from Luochuan loess profile

We describe next two approaches based on what we term the “Residual Trace Approach” (RTA) for paleoprecipitation reconstruction, and demonstrate their application over the past 130 ka in the Luochuan loess profile. The first is the *SUS-approach* where the dust dilution effect on pedogenic susceptibility is considered. The second is $^{10}\text{Be-approach}$, which arose from ^{10}Be production rate reconstruction studies (Zhou et al, 2007a, 2007b, 2010a, 2010b). In the $^{10}\text{Be-approach}$, the influences of both atmospheric ^{10}Be production rate and loess dust flux on the wet deposited ^{10}Be records are considered.

2.1 *SUS-approach*

In the *SUS-approach* we use magnetic susceptibility

$SUS(M) = SUS(D, P)$ (Fig.1b) and dust flux D (Fig.1a) to reconstruct precipitation P at Luochuan for the past 130 ka. As stated above, this approach is different from previous methods that ignored dilution effects of the loess component on the pedogenic susceptibility (Maher et al, 1994; An and Sun, 1995; Sun et al, 1995; Han et al, 1996), and considers the dilution effect of the dust deposition on the pedogenic susceptibility $SUS(P)$.

We first assume that the dustfall-induced susceptibility $SUS(D)$ is independent of precipitation and is homogenous in both its spatial and temporal distributions (Zhou et al, 2007a), it is reasonable to use the measured $SUS(M) = SUS(D, P)$, instead of the $SUS(P)$ for precipitation reconstruction, since the pure $SUS(P)$ is difficult to be extracted from the total $SUS(M)$.

A linear regression of $SUS(M)$ vs. D for the Luochuan loess profile during the past 130 ka is:

$$SUS(M)_e = -11.78D + 294.30, R^2 = 0.64 \quad (1)$$

According to Mean Value Concept (MVC) (Zhou et al, 2007b), the estimated $SUS(M)_e$ is determined by the varying dust flux D under the average precipitation \bar{P} for the past 130 ka. The negative slope of the regression line reflects the dilution effect of D on the magnetic susceptibility.

We can then compute residual values compared to those for \bar{P} as:

$$\Delta SUS(\Delta P) = SUS(M) - SUS(M)_e \quad (2)$$

These are fluctuations of pedogenic susceptibility caused by changes in monsoon precipitation relative to the mean precipitation $\Delta P = P - \bar{P}$ (Zhou et al, 2007b).

We next assert that the residual $\Delta SUS(\Delta P)$ should be linearly correlated to precipitation variations ΔP about the mean, \bar{P} ,

$$\begin{aligned} \Delta SUS(\Delta P) &= m\Delta P + n \\ \Delta SUS(\Delta P) &= m(P - \bar{P}) + n \end{aligned} \quad (3)$$

Thus the absolute precipitation at age T is:

$$P_T = \frac{\Delta SUS(\Delta P)_T - n + m\bar{P}}{m} \quad (4-1)$$

And the absolute precipitation during the present day T_0 is:

$$P_{T_0} = \frac{\Delta SUS(\Delta P)_{T_0} - n + m\bar{P}}{m} \quad (4-2)$$

The [0, 1] normalization is introduced in order to delete the unknown constants in (4).

$$\begin{aligned} \langle P \rangle_T &= \frac{P_T - P_{\min}}{P_{\max} - P_{\min}} \\ &= \frac{\Delta SUS(\Delta P)_T - \Delta SUS(\Delta P)_{\min}}{\Delta SUS(\Delta P)_{\max} - \Delta SUS(\Delta P)_{\min}} \end{aligned} \quad (5-1)$$

$$\begin{aligned} \langle P \rangle_{T_0} &= \frac{P_{T_0} - P_{\min}}{P_{\max} - P_{\min}} \\ &= \frac{\Delta SUS(\Delta P)_{T_0} - \Delta SUS(\Delta P)_{\min}}{\Delta SUS(\Delta P)_{\max} - \Delta SUS(\Delta P)_{\min}} \end{aligned} \quad (5-2)$$

where the symbol $\langle \rangle$ denotes the normalized precipitation value, and the footprint 'max' and 'min' is the maximum and minimum residual or P within the regression interval.

Then the ratio of (5-1) to (5-2) would be the relative precipitation to be reconstructed to the present, if the smallest precipitation is $P_{\min} = 0$ within the regression interval.

$$\begin{aligned} P_T &= \frac{\langle P \rangle_T}{\langle P \rangle_{T_0}} = \frac{P_T - P_{\min}}{P_{T_0} - P_{\min}} \\ &= \frac{\Delta SUS(\Delta P)_T - \Delta SUS(\Delta P)_{\min}}{\Delta SUS(\Delta P)_{T_0} - \Delta SUS(\Delta P)_{\min}} \frac{P_{\min} = 0}{P_{\min} = 0} \\ &= \frac{P_T}{P_{T_0}} \end{aligned} \quad (6)$$

where the present relative precipitation $P(T_0) = 1$.

The next step is how to determine the $\Delta SUS(\Delta P)_{\min}$ corresponding to the $P_{\min} = 0$, that will be discussed in section 2.3.

2.2 ^{10}Be -approach

In ^{10}Be -approach, we will extract the precipitation P signals from the measured $\text{Be}(M) = \text{Be}(D, P, Pr)$ (Fig.1c) by using both the loess dust flux D (Fig.1a) and the reconstructed atmospheric ^{10}Be production rate Pr (Fig.2) synthesized from two Pr curves reconstructed from the Luochuan and Xifeng loess ^{10}Be records (Zhou et al, 2010a) which are closely comparable with the calculated ^{10}Be production rate from marine ^{10}Be (Christl et al, 2010) and SINT 800 paleointensity records (Guyodo and Valet, 1999).

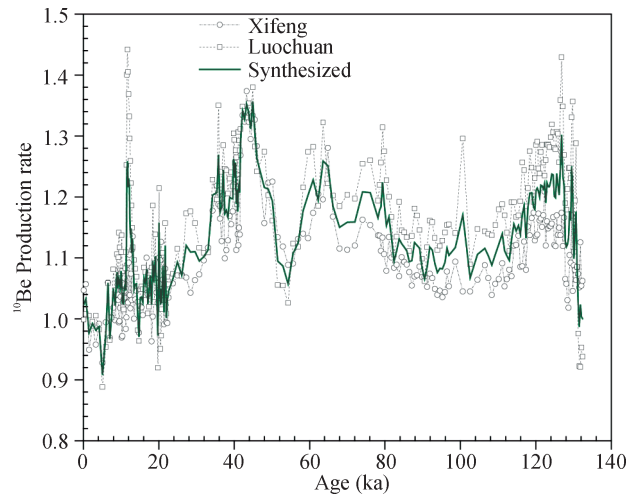


Fig.2 The reconstructed ^{10}Be production rate Pr curve synthesized from two Pr curves reconstructed from the past 130 ka of Luochuan and Xifeng ^{10}Be records (Zhou et al, 2010a)

In the ^{10}Be -approach (Zhou et al, 2014a), we first carried out binary linear regression of $\text{Be}(M)$ with Pr and D over the past 130 ka Luochuan loess profile:

$$\begin{aligned} \text{Be}(M)_e &= 103.48Pr - 14.84D + 341.70 \\ &= \text{Be}(Pr, D, \bar{P}), R^2 = 0.64 \end{aligned} \quad (7)$$

where the estimated value $\text{Be}(M)_e$ is determined by

varying Pr and D under the average precipitation \bar{P} of the past 130 ka according to the MVC (Zhou et al, 2007b) and the dust dilution effect is apparent in the negative slope before D in equation (7).

Next, we obtain the residual:

$$\begin{aligned} \Delta Be(\Delta P) &= Be(M) - Be(M)_e \\ &= Be(D, P, Pr) - Be(D, \bar{P}, Pr) \end{aligned} \quad (8)$$

which is the loess ^{10}Be concentration fluctuations caused by the precipitation variations ΔP relative to the average \bar{P} of past 130 ka according to MVC.

Similar to (3)~(6), the ratio in (9) would be the relative precipitation to be reconstructed to the present, if the smallest precipitation is $P_{min} = 0$ within the regression interval.

$$\begin{aligned} P(T) &= \frac{\langle P \rangle_T}{\langle P \rangle_{T_0}} = \frac{P_T - P_{min}}{P_{T_0} - P_{min}} \\ &= \frac{\Delta Be(\Delta P)_T - \Delta Be(\Delta P)_{min}}{\Delta Be(\Delta P)_{T_0} - \Delta Be(\Delta P)_{min}} \frac{P_{min} = 0}{P_{min} = 0} \\ &= \frac{P_T}{P_{T_0}} \end{aligned} \quad (9)$$

where the present relative precipitation $P(T_0)=1$.

The next step is how to determine the $\Delta Be(\Delta P)_{min}$ corresponding to the $P_{min} = 0$, that will be discussed in section 2.3.

2.3 Normalization and Scaling

As mentioned above, the ratios in (6) and (9) would be relative precipitation when reconstructed to the present. If the smallest precipitation within the regression interval is $P_{min} = 0$ then the corresponding residual would be $\Delta y_{min}(\Delta SUS(\Delta P)_{min}$ or $\Delta Be(\Delta P)_{min})$ (10),

$$\begin{aligned} P(T) &= \frac{\langle P \rangle_T}{\langle P \rangle_{T_0}} = \frac{P_T - P_{min}}{P_{T_0} - P_{min}} \frac{P_{min} = 0}{P_{min} = 0} \\ &= \frac{P_T}{P_{T_0}} = \frac{\Delta y_T - \Delta y_{min}}{\Delta y_{T_0} - \Delta y_{min}} \end{aligned} \quad (10)$$

Under the limiting condition that precipitation $P=0$, the corresponding composition of the pedogenic susceptibility in loess would be $SUS(P)=0$, and the measured contemporary total susceptibility $SUS(M)$ is the smallest and is only related to dustfall-induced susceptibility, i.e. $SUS(M)=SUS(D)$. According to the comparison of loess magnetic susceptibility versus

coercivity (Evans and Heller, 2001) from a wide range of locations on the Chinese Loess Plateau for the last 135 ka, the endmember of high coercivity represents a dry dust component of loess susceptibility. We note the corresponding $SUS(D) \approx 25 \times 10^{-8} \text{ (m}^3 \cdot \text{kg}^{-1}\text{)}$ (driest period) (Zhou et al, 2007a).

Consequently, we can find the age corresponding to the smallest susceptibility $SUS(M) \leq 25 \text{ (} 10^{-8} \text{ m}^3 \cdot \text{kg}^{-1}\text{)}$, and we can obtain the corresponding residual Δy_{min} from the regression equation, i.e., $\Delta SUS(\Delta P)_{min}$ in *SUS-approach*, $\Delta Be(\Delta P)_{min}$ in ^{10}Be -*approach*. If the measured datum error is moderate, the residual Δy_{min} ($\Delta SUS(\Delta P)_{min}$ or $\Delta Be(\Delta P)_{min}$) should be the smallest (most negative) within the concerned regression interval. With the value of $\Delta SUS(\Delta P)_{min}$ or $\Delta Be(\Delta P)_{min}$, the relative precipitation to the present can be reconstructed from equations (6) or (9).

On the other hand, it has been acknowledged through modern observation that the average precipitation at present is about $P_{T_0} \approx 650 \text{ mm}$ in Luochuan, thus, we can calculate the absolute precipitation through scaling the present relative precipitation to $P_{T_0} = 650 \text{ mm}$, noting the present relative precipitation $P(T_0)=1$.

$$\begin{aligned} P_{T_0} \approx 650 \text{ mm} &\xrightarrow{\text{scale}} \frac{P(T_0)}{650} = \frac{1}{650} \\ &= \frac{P(T)}{P_T} \rightarrow P_T = 650P(T) \end{aligned} \quad (11-1)$$

Or through scaling the present normalized precipitation $\langle P \rangle_{T_0}$ to 650 mm (Zhou et al, 2014a), which will introduce the $\Delta SUS(\Delta P)_{max}$ or $\Delta Be(\Delta P)_{max}$.

$$\begin{aligned} P_{T_0} \approx 650 \text{ mm} &\xrightarrow{\text{scale}} \frac{\langle P \rangle_{T_0}}{650} \\ &= \frac{\langle P \rangle_T}{P_T} \rightarrow P_T = 650 \frac{\langle P \rangle_T}{\langle P \rangle_{T_0}} \end{aligned} \quad (11-2)$$

of which,

$$\langle P \rangle_T = \frac{P_T - P_{min}}{P_{max} - P_{min}} = \frac{\Delta SUS(\Delta P)_T - \Delta SUS(\Delta P)_{min}}{\Delta SUS(\Delta P)_{max} - \Delta SUS(\Delta P)_{min}}$$

in *SUS-approach*, and

$$\langle P \rangle_T = \frac{P_T - P_{min}}{P_{max} - P_{min}} = \frac{\Delta Be(\Delta P)_T - \Delta Be(\Delta P)_{min}}{\Delta Be(\Delta P)_{max} - \Delta Be(\Delta P)_{min}}$$

in ^{10}Be -*approach*.

2.4 Cross check and inter-comparison

The correlation coefficient of the reconstructed precipitation curves (Fig.3 a, b) by the two approaches are 0.96. The relative differences of their average values are 13.0% (0~130 ka) and 12.7% (0~80 ka), and the *RSDs* (relative standard deviation of their difference to the average \bar{P}) are 9.6% (Tab.3).

In order to compare our results with other susceptibility-reconstructed precipitation records, we substituted our measured magnetic susceptibility value $SUS(M)$ (Fig.1b) (or approximate pedogenic $SUS(P)=SUS(M)-25$) into the individual climofunctions introduced by previous studies (Maher et al, 1994; Han et al, 1996; Porter et al, 2001) to calculate the past 130 ka precipitation over the Louchuan loess profile. These results are superimposed on our curves as shown in Fig.3. The differences are apparent, especially at age ranges between 80~110 ka where the alternative curves are higher than ours (Fig.3 c,

d, e).

In our view, the high pedogenic susceptibility during 80~110 ka (Fig.1b) formed through a combination of high precipitation and low dust flux (Fig.1a) rather than by high precipitation alone, so the horizontal sections of the precipitation curves during 80~110 ka should follow a lower trend, such as ours (Fig.3 a, b). The previous approaches follow a trend above these values because they failed to account for the abrupt drop in dust flux from 80~110 ka (Fig.1a).

In addition, our reconstructed precipitation records (Fig.4 a, b) compare well with the $\delta^{18}O$ records from Hulu-Sanbao caves (Fig.4c) (Wang et al, 2001, 2008), which is widely regarded as a reliable record of Asian Monsoon intensity. Like speleothem $\delta^{18}O$ records, ^{10}Be precipitation records in loess during MIS 5 clearly reveal sub-cycles (MIS 5a—MIS 5e) of precipitation changes, providing further proof that our approaches are reliable.

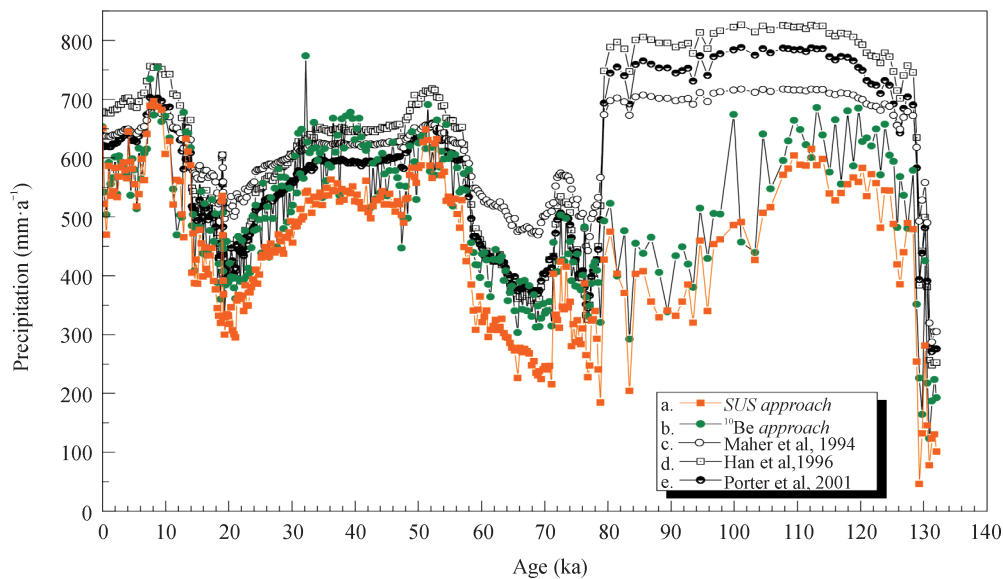


Fig.3 The comparison of the reconstructed precipitation curves by the *SUS*-approach (a) and the ^{10}Be -approach (b) with individual precipitation curves (c-e) reconstructed by substituting our measured magnetic susceptibility values into the climofunctions reported in previous studies

Tab.3 The average precipitation (\bar{P}) and their relative differences (σ , *RSD*) and correlation coefficient (R^2) of the reconstructed precipitation curves by two approaches

	\bar{P} (<i>SUS</i> -approach)	\bar{P} (^{10}Be -approach)	$\frac{\Delta\bar{P}}{\bar{P}}$	Correlation (R^2)	σ	<i>RSD</i>
0~130 ka	440.7	506.3	13.0%	0.92 ($r=0.96$)	48.6	9.6%
0~80 ka	444.4	508.9	14.9%	0.91 ($r=0.96$)	48.7	9.6%

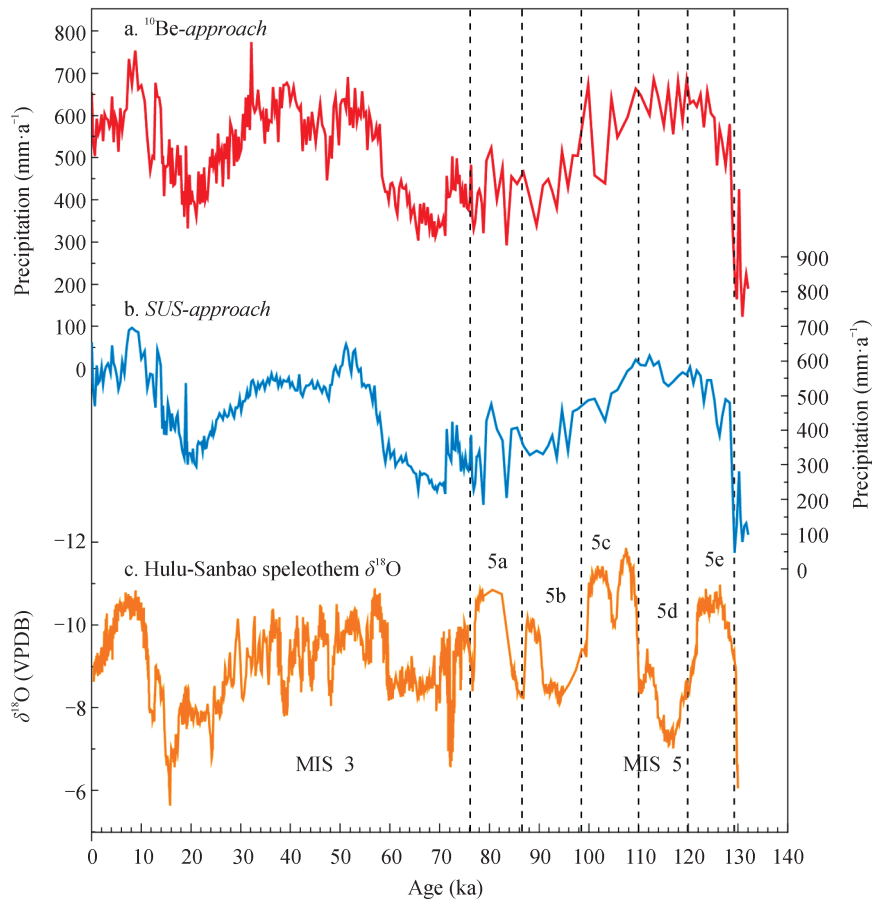


Fig.4 The reconstructed past 130 ka precipitation over the Louchuan loess profile by a) ^{10}Be -approach and b) SUS -approach, and their correlation with speleothem $\delta^{18}\text{O}$ records (c) from Hulu-Sanbao caves (Wang et al, 2001, 2008)

2.5 Summary for the paleoprecipitation reconstruction

Using the loess susceptibility alone for precipitation reconstruction in previous studies based on the traditional trace methods has derived a number of climofunctions which have neglected to include the influence of dust dilution on pedogenic susceptibility, and on the reconstructed precipitation. The paired measurements of loess susceptibility and loess dust flux can be used to reconstruct glacial and interglacial precipitation by using the SUS -approach, in which the dust dilution influence on the reconstructed precipitation is accounted for.

As a byproduct of reconstruction global ^{10}Be production rate (or geomagnetic intensity) reconstruction, we can use the ^{10}Be -approach to reconstruct precipitation over the loess plateau. The coincidence of the reconstructed precipitation curves by the two approaches is marked. Nevertheless, as speculated by previous workers (Heller

et al, 1993; Maher et al, 1994), difficulties are also encountered with the SUS -approach and ^{10}Be -approach in determining precise estimates of dust flux through the loess accumulation rates and the dry bulk density.

3 Mathematical explanation of the “Residual Trace Approach”: Mean Value Concept

Variables $SUS(P, D)$, P , D used in the SUS -approach, or variables $\text{Be}(P, D, Pr)$, (P, D) , Pr used in the ^{10}Be -approach constitute multiple variables $y(x_1, x_2)$, x_1 , x_2 . Other than conventional multivariable regression analysis or traditional tracer research, in the “Residual Trace Approach”, we carry out the linear regression analyses between $y(x_1, x_2)$ and x_1 to remove the effect of x_1 , and then carry out a calculation to quantify the variation due to the second variable x_2 through the calculated residual $\Delta y(\Delta x_2)$.

Usually, the estimated regression equations (1) and (7) are expressed as the only correlation between

$y(x_1, x_2)$ and x_1 .

$$y(x_1, x_2)_e = ax_1 + b \tag{12}$$

Obviously, the second variable x_2 “uninvolved” in regression equation (12), must be a constant x_c in the estimated values $y(x_1, x_2 = x_c)_e$ or on the regression line, otherwise the regression analysis (12) would be meaningless, and the calculated residuals $\Delta y(\Delta x_2)$ are caused only by the difference between the measured x_2 and the constant x_c on the regression line.

How much is the constant x_c on the regression line? According to our study (Zhou et al, 2007b), this constant is taken to be $x_c = \bar{x}_2$, the arithmetic mean value of x_2 over the concerned regression interval. Namely, all x_2 values corresponding to estimated values on the regression line are equal to the arithmetic mean value \bar{x}_2 (Fig.5). This is the root of the MVC (Mean Value Concept) (Zhou et al, 2007b), which can be

further explained from a statistical view as following.

The top and middle panels of Fig.5 are the scatter diagrams of $y(x_1, x_2)$ vs. x_1 (Fig.5a) and $y(x_1, x_2)$ vs. x_2 (Fig.5b) respectively. The decline line in Fig.5a is the regression line of $y(x_1, x_2)$ vs. x_1 and the vertical line in Fig.5b is the constant x_2 line x_c corresponding to the value on the regression line. Even though assuming the complete correlation between $y(x_1, x_2)$ and x_1 and without datum errors, all measured data $y(x_1, x_2)$ are distributed around the two sides of the regression line (Fig.5a). They are located at different distance $\Delta y(\Delta x_2)$ from the regression line depending on the Δx_2 , the deviation of the x_2 values from the constant value x_c (Fig.5b). No matter whether the correlation between $y(x_1, x_2)$ and x_2 is linear or nonlinear, the further the Δx_2 , the bigger the $\Delta y(\Delta x_2)$, and *vice versa*.

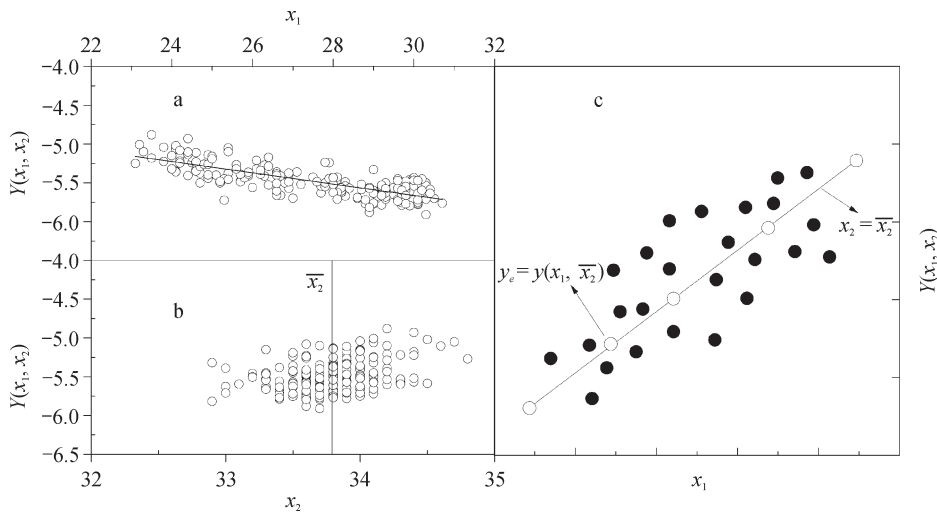


Fig.5 Scatter diagrams of $y(x_1, x_2)$ vs. x_1 (a) and $y(x_1, x_2)$ vs. x_2 (b) as well as the regression line (c) with the arithmetic mean value \bar{x}_2 .

If we define the $\Delta y(\Delta x_2)$, the deviation from the regression line caused by the Δx_2 , as a “residual”, like the conventionally defined residual in statistics due to datum error or incomplete similarity correlation, the regression equation derived by computer programs must be determined in compliance with the minimum of the sum of the “residual” square $\Delta y(\Delta x_2)^2$ or the deviation square Δx_2^2 according to the well-known principle of least

square method, applicable to linear correlations. Moreover, the statistics indicates that the summation of the squares of the deviation from arithmetic mean value is the least among the sum of various deviation squares. Thus the constant x_c on the regression line (Fig.5c) or on the vertical line (Fig.5b) must be the arithmetic mean value \bar{x}_2 so as to meet the minimum of the sum of the “residual” squares $\Delta y(\Delta x_2)^2$ or the deviation squares Δx_2^2 . That is the virtual Mean

Value Concept (MVC) deduced from the statistical point of view. The more the number of specimens, the more accurate the MVC.

According to the MVC, a linear regression of a multivariable system, such as $y(x_1, x_2)$ vs. x_1 , is carried out around the average \bar{x}_2 , and the estimated value $y(x_1, x_2)$ of the regression equation (12) is the correlation between $y(x_1, x_2)$ and x_1 under the condition of constant \bar{x}_2 (Fig.5c).

With introduction of the MVC, we realize the residual in RTA,

$$\Delta y(\Delta x_2) = y(x_1, x_2) - y(x_1, \bar{x}_2) = y(x_1, x_2) - y(x_1, \bar{x}_2) \quad (13)$$

is the variations of $y(x_1, x_2)$ caused by the Δx_2 , variation of x_2 relative to its average value \bar{x}_2 within concerned regression interval, which becomes the mathematic connotation of the “Residual Trace Approach”.

4 Other successful application examples of the “Residual Trace Approach”

By taking the loess susceptibility as climate (P, D) proxy, this new approach has successfully been applied to reconstruct the past 80 ka, 130 ka paleogeomagnetic intensities by using the ^{10}Be records in Luochuan and Xifeng loess profiles (Zhou et al, 2007a, 2010a). By using this approach, we have determined the Brunhes/Matuyama (B/M) geomagnetic reversal at circa 780 ± 3 ka BP in Xifeng and Luochuan loess profiles, this timing

is synchronous with the B/M reversal timing seen in marine records, facilitating the resolution of the long standing debate about the discrepancy of the B/M magnetic records between Chinese loess and marine sediments by paleomagnetic studies (Zhou et al, 2014b).

In addition, taking the radioisotope ^{90}Sr as proxy of the sea surface temperature, we have applied this new approach to quantitatively reconstruct the past 90 years’ sea salty in the Xisha and Hainan islands with $\delta^{18}\text{O}$ (Song, 2006) records.

There is no doubt that the “Mean Value Concept” based “Residual Trace Approach” has opened a new way in environment tracing studies. The differences of the developed “Residual Trace Approach” from the traditional trace method are compared in tab.4, both of which can be applied to the trace research under the respect appropriate condition and with its own advantage and disadvantage, and the “Residual Trace Approach” is especially suitable to the trace research for a multivariable geosystem where all variables are changeable and their distribution have been known except the one to be reconstructed. However, it is important for RTA that the linear correlation between the dependent variable y and independent variables $x_1, x_2 \dots$ should be high, the higher the linear correlation, the more accurate the traced/ reconstructed results.

Tab.4 Comparison of the “Residual Trace Approach” with the traditional trace approach

Tracing x_2 from $y(x_1, x_2)$	Traditional trace approach	Residual Trace Approach
regression sequence	x_2 vs. $y(x_1, x_2)$	$y(x_1, x_2)$ vs. x_1
regression equation	mono-linear regression	mono-element or mul-ti-element
regression manner	nonlinear regression	linear regression
variables involved in regression	x_2 & y	x_1 & y
the other variable ‘un-involved’ into the regression calculation	setting or assuming the other variable x_1 to be constant	the other variable x_2 is changing and has been known, but the x_2 on the regression line has its arithmetic mean value over regression interval (MVC)
regression interval of derived equation	the latest ages of the concerned period	the whole concerned period
traced age range	extended to far beyond regression interval	confined in the whole concerned regression interval
trace approach	climofunction	residual + normalization

References

- 孙东怀, 周杰, 吴锡浩. 1995. 全新世气候适宜期黄土高原及黄土/沙漠过渡区年降水量的初步恢复 [J]. *中国沙漠*, 15: 339–344. [Sun D H, Zhou J, Wu X H. 1995. Preliminary reconstruction of annual rainfall in loess plateau and loess-desert transitional regions in suitable climatic period of Holocene [J]. *Journal of Desert Research*, 15: 339–344.]
- 周卫健, 孔祥辉, 鲜锋, 等. 2010b. 中国黄土 ^{10}Be 重建古地磁场变化史的初步研究 [J]. *地球环境学报*, 1(1): 20–27. [Zhou W J, Kong X H, Xian F, et al. 2010b. Preliminary study on the reconstruction of the palaeogeomagnetic intensities by ^{10}Be in Chinese loess [J]. *Journal of Earth Environment*, 1(1): 20–27.]
- An Z S, Sun D H. 1995. Discussion on the monsoon variation over the Loess Plateau in the Last Glacial Cycle [M]. Beijing: Science Press.
- Beer J, Shen C D, Heller F, et al. 1993. ^{10}Be and magnetic susceptibility in Chinese Loess [J]. *Geophysical Research Letters*, 20: 57–60.
- Caillet S, Arpagaus P, Monna F, et al. 2001. Factors controlling ^7Be and ^{210}Pb atmospheric deposition as revealed by sampling individual rain events in the region of Geneva, Switzerland [J]. *Journal of Environmental Radioactivity*, 53: 241–256.
- Christl M, Lippold J, Steinhilber F, et al. 2010. Reconstruction of global ^{10}Be production over the past 250 ka from highly accumulating Atlantic drift sediments [J]. *Quaternary Science Review*, 29: 2663–2672.
- Evans M E, Heller F. 2001. Magnetism of loess/palaeosol sequences: recent developments [J]. *Earth-Science Reviews*, 54: 129–144.
- Guyodo Y, Valet J P. 1999. Global changes in intensity of the Earth's magnetic field during the past 800 kyr [J]. *Nature*, 399: 249–252.
- Han J M, Lu H Y, Wu N Q, et al. 1996. The magnetic susceptibility of modern soils in China and its use for paleoclimate reconstruction [J]. *Studia Geophysica et Geodaetica*, 40: 262–275.
- Heller F, Shen C D, Beer J, et al. 1993. Quantitative estimates of pedogenic ferromagnetic mineral formation in Chinese loess and palaeoclimatic implications [J]. *Earth and Planetary Science Letters*, 114: 385–390.
- Ishikawa Y, Murakami H, Sekine T, et al. 1995. Precipitation scavenging studies of radionuclides in air using cosmogenic ^7Be [J]. *Journal of Environmental Radioactivity*, 26: 19–36.
- Kukla G, Heller F, Liu X M, et al. 1988. Pleistocene climates in China dated by magnetic susceptibility [J]. *Geology*, 16: 811–814.
- Maher B A, Thompson R, Zhou L P, et al. 1994. Spatial and temporal reconstructions of changes in the Asian palaeomonsoon: A new mineral magnetic approach [J]. *Earth and Planetary Science Letters*, 125: 461–471.
- Porter S C, Hallet B, Wu X H, et al. 2001. Dependence of near-surface magnetic susceptibility on dust accumulation rate and precipitation on the Chinese Loess Plateau [J]. *Quaternary Research*, 55: 271–283.
- Shen C D, Beer J, Heller F, et al. 2000. ^{10}Be -susceptibility model and quantitative estimates of pedogenic ferromagnetic material flux in Chinese loess [J]. *Nuclear Instruments and Methods in Physics Research Section B: Beam Interactions with Materials and Atoms*, 172: 551–554.
- Song S H. 2006. Reconstruction of climatic history based on coral in South China Sea and the related data analysis method [D]. Beijing: Graduate University of Chinese Academy of Sciences.
- Wallbrink P J, Murray A S. 1994. Fallout of ^7Be in South Eastern Australia [J]. *Journal of Environmental Radioactivity*, 25: 213–228.
- Wang Y J, Cheng H, Edwards R L, et al. 2001. A high-resolution absolute-dated Late Pleistocene monsoon record from Hulu Cave, China [J]. *Science*, 294: 2345–2349.
- Wang Y J, Cheng H, Edwards R L, et al. 2008. Millennial- and orbital-scale changes in the East Asian monsoon over the past 224,000 years [J]. *Nature*, 451: 1090–1093.
- Zhou W J, Priller A, Beck W, et al. 2007a. Disentangling geomagnetic and precipitation signals in an 80-kyr Chinese loess record of ^{10}Be [J]. *Radiocarbon*, 49: 139–160.
- Zhou W J, Chen M B, Xian F, et al. 2007b. The mean value concept in mono-linear regression of multi-variables and its application to trace studies in geosciences [J]. *Science in China Series D: Earth Sciences*, 50: 1828–1834.
- Zhou W J, Xian F, Beck W, et al. 2010a. Reconstruction of 130-kyr relative geomagnetic intensities from ^{10}Be in two Chinese loess sections [J]. *Radiocarbon*, 52: 129–147.
- Zhou W J, Xian F, Du Y J, et al. 2014a. The last 130ka precipitation reconstruction from Chinese loess ^{10}Be [J]. *Journal of Geophysical Research: Solid Earth*, 119: 191–197.
- Zhou W J, Beck W, Kong X H, et al. 2014b. Timing of the Brunhes-Matuyama magnetic polarity reversal in Chinese loess using ^{10}Be [J]. *Geology*, 42: 467–470.